Universitat Autònoma de Barcelona

Departament d'Enginyeria Electrònica

Energy management, wireless and system solutions for highly integrated implantable devices

Memòria presentada per

Jordi Parramon i Piella

per optar al grau de

Doctor en Enginyeria Electrònica

Departament d'Enginyeria Electrònica

Edifici Cn
08193 Bellaterra (Barcelona). Spain
Tel.: 93 581 31 83
FAX: 93 581 13 50
E-mail: d_eng.electronica@uab.es

Universitat Autònoma de Barcelona

Departament d'Enginyeria Electrònica

La Dra. Elena Valderrama Valles, Catedràtica d'Informàtica de la Universitat Autònoma de Barcelona,

CERTIFICA

Que la memòria **"Energy management, wireless and system solutions for highly integrated implantable devices"** que presenta Jordi Parramon i Piella per optar al grau de Doctor en Enginyeria Electrònica, ha estat realitzat sota la seva supervisió.

Bellaterra, Desembre del 2001

Dra. Elena Valderrama Valles

ABSTRACT

In the recent years a very challenging product line of the biomedical industry has emerged, with a fast-growing market and very promising future: implantable electronic devices. Reliability, miniaturization and life-time are key problems of this business. New technologies, especially microelectronics, are capable of giving answers to such challenges.

The following thesis describes a variety of solutions developed in the framework of several projects in terms of power management (with both RF and battery powered approaches), high-bandwidth bi-directional wireless communication and system design and architecture to be applied into highly integrated implantable devices.

RESUM

En els últims anys una nova línia de productes dins la indústria biomèdica a començat a prendre embranzida, presentant un elevat creixement i unes perspectives de futur molt encoratjadores: dispositius electrònics implantables. Els problemes més crítics es troben en el fet que els implants han de ser molt segurs, de tamany reduït i han de tenir un temps de vida llarg. Només les noves tecnologies, entre elles especialment la microelectrònica, són capaces de donar resposta a aquests reptes.

La present tesi doctoral descriu una varietat de solucions desenvolupades en el marc de diferents projectes enfocades a solucionar el problema del subministrament d'energia (ja sigui usant camps electromagnètics o bateries), la comunicació d'alta velocitat amb el món exterior i d'altres problemes a nivell de sistema, sempre en el marc de dispositius electrònics altament integrables.

AGRAïMENTS:

Des del dia en que com a estudiant no graduat vaig rebre la “proposición indecente” en paraules textuals de l’Elena Valderrama per formar part del projecte europeu INTER (i enllestir el meu projecte final de carrera d’Enginyeria Electrònica) fins avui mateix que estic vivint a Califòrnia, m’han passat força coses tant a nivell professional com personal. Entre altres aquesta tesi doctoral que és el resultat explícit de la feina feta durant una sèrie d’anys sobretot al Centre Nacional de Microelectrònica, en particular dins el grup d’aplicacions biomèdiques. Voldria expressar primer de tot el meu agraïment a l’Elena, no només pel fet d’acceptar dirigir-me la tesi, sinó també pel privilegi que suposa haver estat treballant al seu costat. Un altre motiu d’agraïment i que comparteix amb el director del CNM Francesc Serra-Mestres es remunta a quan vaig començar amb tot això de l’electrònica. Durant el primer curs, jo anava molt atrafegat amb la simultaneïtat d’estudis amb Ciències Físiques. I més d’una vegada em vaig plantejar deixar-ho. Van ser les seves classes en gran mesura les que van motivar-me a continuar.

Vull també donar les gràcies a la Tere Osés, la Rosa Villa i en Jordi Aguiló del CNM-GAB per creure i seguir creient que la microelectrònica i la biomedicina poden tenir molt a veure. De l’UAB voldria donar les gràcies tant a la Núria Barniol com a en Joan Oliver per haver–me ajudat valuosament als inicis del doctorat. Agraeixo tant a David Marín que va continuar la feina de telemetria quan jo vaig marxar als Estats Units, com a Pacu Serra-Graells, Ivan Erill, i en general a tots els companys del CNM per haver compartit amb ells tantes hores.

De les meves dues estades i posterior col.laboració amb l’institut Fraunhoffer de biomedicina IBMT de Sant Ingbert-Alemanya voldria agrair especialment a l’Uwe Meyer per invitar-me cordiarlment al seu centre. També un agraïment per Oliver Scholz, Hasnsjoerg Beutel i altres companys de centre amb qui vaig poder compartir treball i amistat.

De la meva estada d'un any als Estats Units a cavall entre la Case Western Reserve University i la The University of Memphis, voldria agrair especialment el mentoratge del professor Michael R. Neuman, aixi com poder haver treballat amb B.D. Pendley i rebut ajuda de l'estudiant Chat Rowan.

Del projecte ITUBR vull agrair a tots els centres integrants l'esforç que van realitzar i que en gran mesura ha fet possible aquesta tesi doctoral. En particular pel que fa referència al desenvolupament de la unitat externa de telemetria i packaging voldria agrair el treball de Julio Arzuaga i demés membres del CCC d'Uruguay. També cal agrair tant a la Universidad de Los Andes amb el professor Antonio García-Rozo com a la Fundación Cardio-infantil de Bogotà amb el professor Juan Carlos Briceño per haver col.laborat decisivament en l'obtenció de resultats in-vivo. Però per sobre de tot una cosa he d'agrair al Professor García-Rozo: el fet d'haver-se posat malalt dies abans de celebrar-se una reunió del projecte ITUBR a Mèxic DF. Per estranyes circumstàncies de la vida aquest fet va fer possible conèixer la Isabel que ara és la meva dona. De qui per cert he d'agrair (o mes aviat lamentar) les seves despiatades correccions a la meva pobra gramàtica anglesa.

Cal també donar gràcies a la Generalitat de Catalunya per haver-me pagat el sou mitjantcant una beca pre-doctoral FPI durant els anys de doctorat i també pel fet d'ajudar-me incondicionalment a obtenir del govern espanyol una carta de "no objecció" per tal que pogués incorporar-me a una companyia de Califòrnia sense haver d'estar els pre-establerts dos anys a Espanya per poder canviar el meu estatus de visat.

De la companyia Advanced Bionics Corporation, on continuo podent gaudir de la recerca en micro-dispositius electrònics implantables voldria agrair especialment la insistència del meu director Matt Haller, per tal que acabes d'escriure la tesi.

Ja per enllestir, voldria donar les gràcies a l'Amàlia, a tots els meus amics, i a tots els membres de la meva família, en particular als meus pares.

ACKNOWLEDGEMENTS:

Since the day I received, as an undergraduate student, the proposal from Elena Valderrama to join the European INTER project (and finish my EE final project) until today that I am living in California, many things have happened to me in both the personal and professional level. Among them the following doctoral thesis, that is the result of the work done mainly in the CNM-, in particular in the biomedical applications group. I would like first of all, to thanks Elena, not only because she accepted me as a PhD student but also because it was truly a pleasure to work with her. Another reason that I must acknowledge from her, in that case shared with the director of the CNM Francesc Serra-Mestres, is related with the beginning of my studies in engineering. During the first year, I was really busy trying to keep up with the EE at the same time than with Physics. And more than once I had second thoughts about just giving up. Their teaching help me a lot to keep going.

I would like to thanks Tere Oses, Rosa Villa and Jordi Aguilo, from CNM-GAB to believe that microelectronics and biomedical applications may have quite a future together. From the UAB I thank Nuria Barniol and Joan Oliver because they were the first to help me valuably in the beginning of my work. I also acknowledge David Marin to continue the work I did, right after my departure to the States, as well as Pacu Serra-Graells, Ivan Erill and in general all the friends and colleagues of the CNM.

From my two visits to the Fraunhoffer institute of biomedicine IBMT-Germany, I would like to thanks Uwe Meyer to be so kind to accept me there. As well as Oliver Scholz, Hansjoerg Beutel and other colleagues from whom I was able to share work and friendshipness.

During my thesis, I spend one year in the US working as a research visitor at Case Western Reserve University and at The University of Memphis. All this was possible thanks to professor Mike R. Neuman who kindly accept me in his group. I also appreciate

the possibility to work with B.D. Pendley and with the undergraduate student Char Rowan that helped me valuably.

From the ITUBR project I would like to thank every single center involved in the effort that made possible this thesis. In particular related of the external controller development I thank Julio Arzuaga and the rest of the people from CCC of Uruguay. I also thank the Universidad de Los Andes with professor Antonio Garcia-Rozo and the Fundacion Cardio Infantil with professor Juan Carlos Bricenno of Colombia whose help was decisive in order to obtain in-vivo results. But above all, I thank professor Garcia-Rozo for one thing: the fact he got ill a few days before a meeting project was about to start in Mexico City. This made possible to meet Isabel who is now my wife. And of which I have to thank (or maybe regret) her merciless correction to my poor English grammar.

I would like to thank the Catalan government who sponsored my PhD through a full time grant with the FPI program, and also because it helped me unconditionally to obtain from the Spanish government a “no-objection” letter, that allowed me to join a US company without having to wait the required two years in Spain, due to my immigration visa issues.

I also thank Advanced Bionics Corporation, where I continue to have the pleasure to work with implantable micro-systems and specially Matt Haller, due to his constant insistence in reminding me that I should finish the thesis.

I finally thank to Amalia, to all my friends and my family, and especially my parents.

TABLE OF CONTENTS

LIST OF FIGURES

LIST OF TABLES

CHAPTER ONE

INTRODUCTION

1.1 OVERVIEW OF IMPLANTABLE ELECTRONIC DEVICES

In the recent years a very challenging product line of the biomedical industry has emerged, with a fast-growing market and a even more promising future: implantable electronic devices.

Surprisingly enough the concept of using electricity for medical purposes is not a new idea. Roman physicians in the early years after the birth of Christ recommended the electrical discharge of the torpedo fish for the treatment of headache and gout [1]. Volta and others made important contributions in the understanding of the relationship between electricity and biology, but we had to wait many years to see these old concepts to become part of standard therapy in modern medicine in the form of implantable electronic devices.

The first and probably the most successful implantable electronic device up to date is the pacemaker. Like all other implantable applications was initially implemented with external/surface electrodes in the nineteen thirties [2]. The second generation was a partially implantable system with leads coming out of the skin [3] but discomfort and especially risk of infection were major problems. So finally the last and obvious step was to create a fully implantable pacemaker. By mid 1950s [4], Dr. Rune Elmqvist designed the world's first implantable pacemaker and in late fifties Arn Larsson was the lucky recipient of the first implanted pace. He was a forty-three years old patient who suffered from life-threatening Adams-Stokes seizures. His condition was so bad that it required thirty resuscitations per day. Doctor Senning implanted this pacemaker on October 8, 1958. Mr. Larson had no complications and was still leading an active life by 1995 [5]. Nowadays approximately 600,000 pacemakers are implanted annually and an estimated 3,000,000 people are living with functional pacemakers. The number of

patients receiving pacemakers is increasing at a rate of about 8% per year as the population ages. The current market for cardiac pacemakers is around $3.36 billion/year.

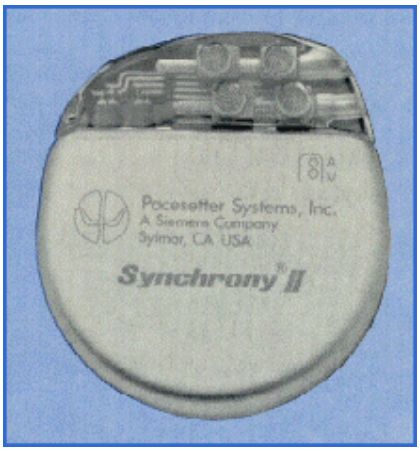

Figure 1-1. Commercial pacemaker (courtesy of Pacesetter)

Following the pacemaker, a second implantable device was coming on the way: implantable defibrillator. During late 60s the first of its kind was developed by Dr. Micheal Mirowski [6]. Since then, this type of device has been very successful, with a typical annual growth of 20-30% toping above 100,000 units per year. Even though these two applications are clearly the "driving force" of the biomedical electrical implant business, new emerging technologies/applications are coming along which can potentially revolutionize certain areas of the medicine. Among others, I would mention the new line of implantable electrical neuromodulation devices and other neuroprosthesis as well as implantable drug delivery systems.

The key concept of electrical neuromodulation is to develop an interface between the nervous system and an electronic device. Learning how to do it is a combination of electrode, electronics and packaging technologies, where experts in heterogeneous fields like material science, microelectronics, electrochemists, biomedicine, cybernetics, etc work together. Interacting bi-directionally with the nervous system opens a door towards new ways of treating diseases that have some neurological basis. In the group of sensory prosthesis the cochlear implant is the most accomplished example. The first direct stimulation of the auditory nerve in man was carried out by Lundber in 1950 and later by Djourno and Eyries in 1957 [7]. Nowadays

the technology has improved so much (better electrodes, more channels, better signal processing) that state-of-the-art cochlear implants (like the one in *Figure 1-2*) may even provide the so called "super-hearing" where patients can hear even better than normal people under certain noise conditions. This technology certainly changes the life of many people. In the photograph bellow a little girl with a facial expression between joy and surprise the first time in her life that she experienced a sound.

Figure 1-2. Commercial Cochlear implant. Courtesy of Advanced Bionics Corp.

Figure 1-3. Expression of joy/surprise of a little girl the first time she heard a sound.

In the same path but with substantially more way to go are the visual prosthesis. Different approaches of how to interface with the visual cortex (either through retina stimulation [8] [9] [10], through the optical nerve [11] [12] or directly stimulating the cortex [13] [14]) are currently under development. Still within the electrical neuromodulation business a set of ambitious large-market applications are being pursued. Among others applications to treat urinary incontinence [15][16], pain management [17], movement disorders [18], Parkinson's disease [19], depression, etc. are also under way with a perspective of a market of vast proportions, that will be able to improve the life quality of millions.

Implantable drug delivery systems are also experiencing a substantial growth recently. Developments in micro-dose delivery devices and specially a huge and growing diabetic population are moving forward this field. An example of this is the so-called artificial pancreas, that would replace completely the functionality of the pancreas (segregate insulin when required) with an implantable insulin pump in conjunction with a glucose sensor [20]. With this new device, occasional refills (maybe

once a month) of a transcutaneous chemical container will be the only activity required by the type I diabetes patients.

In general, all these devices have some kind of bio-compatible body-to-electronics interface (electrodes, sensors, ...) with two major activities : (1) modulating locally the electric field (*current or voltage stimulation*) or delivering chemical substances (*micro-dose delivery*) and (2) sensing a particular body activity (bio-signals *recording*, biochemical concentration, etc.). In many cases both directions are desirable in order to close the loop and provide a "self-contained" behavior of the implant. As typical example and mentioned earlier, would be the new generation of artificial pancreas: an insulin-injector delivers to the blood flow a controlled quantity of insulin depending on the sensed levels of glucose in the blood. Other close-loop controls can be found for example in the area of FES (Functional Electrical Stimulation): a paralyzed patient can potentially regain control of a limb with the proper sensing and stimulating interfaces to his skeletal muscle system.

For all this kind of old needs, only new emerging technologies can give the clue to solve the difficulties and system complexities and bring up feasible devices. Among all these new technologies with no doubt microelectronics plays a major role.

Within the biomedical industry developing implantable devices, three key-points are a major concern for the engineers: *reliability*, *miniaturization*, and *lifetime*. All these three topics can be handled more effectively if microelectronics, and particularly Application Specific Integrated Circuits (ASICs) technologies are used. Improvement in reliability is assured due to the intrinsic performance in this feature of a monolithic silicon circuit. Moreover custom-made integrated circuits allow a dramatic reduction in the number of of-the-shelf components (System-on-Chip approach), thus leading to a smaller device, which ultimately also improves reliability. Finally, lifetime (explantation is something everyone wants to avoid) can be increased due to power reductions that can hardly be accomplished if a customized chip is not developed.

It is clear that to have a reliable, small and durable device is a mandatory fact in the implant world. In terms of functionality an electronic implant can be described as follows:

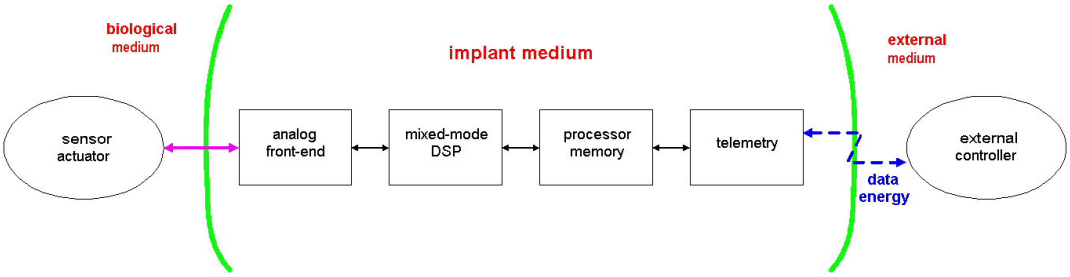

Figure 1-4. General purpose electronic implant

A so-called front-end section interfaces wireless with the external world by means of getting bi-directional data and eventually energy if a batteryless or a rechargeable battery is on board. In the biological-end there are some analog circuits interfacing with the biological media (either for sensing or actuating). And in the middle some sort of DSP (either digital or mixed-mode) is implemented. All these within a hermetically sealed package with possibly some feed-through interfacing the electrodes.

1.2 SCOPE AND STRUCTURE OF THE THESIS

The present thesis describes the work done by the candidate in the scope of the Grup d'Aplicacions Biomèdiques (GAP) within the National Center of Microelectronics of Bellaterra. During the period 1996-1998 the candidate enjoyed a full-time grant (*beca pre-doctoral FPI Generalitat de Catalunya*) including a year visit at Case Western Reserve University (Cleveland, Ohio)/The University of Memphis (Tennessee) during 1998.

The work, developed within several projects, had the continuity necessary to define a compact scope in the field of biomedical implants. In particular solving problems of energy management resulting in the first generation of RF inductive links developed in the CNM-UAB (***chapter two***). Concerning to the wireless data links different solutions are presented for both batteryless (the first high-bandwidth bi-

directional telemetry system developed in the CNM-UAB) or battery operated implants (ultra-low-power operation) (***chapter three***).

It is important to mention that what really rounds the content of the thesis is the actual system-level implementation of the modular solutions presented in both chapters two and three. All this is presented (***chapter four***), where three different systems are depicted involving different levels of development.

The first application is the development of a fully implantable batteryless system for bio-signal recording [21] [22] [23] within the European sponsored project Implantable Telemetry System for Biomedical Research (ITUBR) led by the CNM-Barcelona. The work done by the candidate goes from system specifications, all the way down to implant development (including a custom ASIC conforming a System-on-Chip SoC solution) and parts of an external controller. The involvement also included final "in-vitro" and most importantly "in-vivo" bio-signal recordings, performed in a dog with the device implanted and monitored by a portable external controller/reader that recorded the data. That represented the first fully implantable wireless biomedical device developed in the CNM-UAB to be actually implanted with bio-recordings.

The second application, that included the system level design and a prototype board including two custom ASICs was done in the US in a combined visit at Case Western Reserve University and The University of Memphis. The aim was to obtain a long-term implantable chemical sensor with capability of storage of massive data [24]. "In-vitro" data was also obtained. As opposed to the ITUBR device, a battery was used in here. Therefore the lifetime of the device was critical related to the power consumption. Low power solutions (in system level as well as modular level) were mandatory.

Finally, the third system-level work was not targeting any specific application. The goal, re-using the existing modular hardware developed previously, was to create a single chip to be used in any biomedical implant [25] offering a solution to energy and data needs. The chip was created within the CNM-GAB with a collaboration from the IBMT Institute (Fraunhoffer Institute for Biomidicine at St. Ingbert, Germany).

1.3 REFERENCES

[1] McNeal 1977 pp3-35

[2] W. Greatbatch, "Cardiovascular technology: origins of the implantable Cardiac Pacemaker," *The Journal of the Cardiovascular Nursing* Vol. 5(3), pp.80-85, April 1991.

[3] K.A. Ellenbogan, Cardiac Pacing, Chapter 1, pp. 1-10, Blackwell Scientific Publications, 1992.

[4] Anonymous, "Implantable electronic pace-makers," *The Journal of Medical Electronics*, Vol. 1, pp.15-16, 1962.

[5] R.D Gold, "Cardiac pacing-from then to now," *Medical Intsrumentation*, Vol. 18(1), pp. 15-21, Jan-Feb 1984.

[6] D.W Benson, D.S. Druz, J. Jude, and G. Knickerbocker, "Defibrillation," *Journal of the Association for the Advancement of Medical Instrumentation*, Vol. 3(1), pp.53-69, January 1969

[7] Clark, G.M., Pyman, B.C. and Bailey, Q. (1979) Journal of Laryngology and Otology, 93:215-223

[8] Humayun, M., *et al*. "Visual Perception Elicited by Electrical Stimulation of Retina in Blind Human", *Arch. Ophtalmology*, 114, 40-46, 1996

[9] Liu, W., McGucken, E., Clements, M., DeMarco, S. C, Vichienchom, K., Hughes, C., Humayun, M., de Juan, E., Weiland, J., Greenberg, R., "An Implantable Neuro-stimulator Device for a Retinal Prosthesis", (International Solid-State Circuits Conference, Feb 1999).

[10] Zrenner E, Stett A, Weiss S, Aramant RB, Guenther E, Kohler K, Miliczek K-D, Seiler MJ, Haemmerle H (1999). Can subretinal microphotodiodes successfully replace degenerated photoreceptors? Vision Research 39: 2555-2567

[11] C. Veraart, C. Raftopoulos, D. Pins, J. Delbeke, J.T. Mortimer, M.C. Wanet, G. Michaux, O. Glineur, A. Vanlierde, Optic nerve electrical stimulation in a retinitis pigmentosa blind volunteer. Soc. Neurosci. Abstr., 1998, 24: 2097.

[12] C. Veraart, J. Delbeke, M.-C. Wanet-Defalque, A. Vanlierde, G. Michaux, S. Parrini, O. Glineur, M. Verleysen, C. Trullemans, T. Mortimer, Selectve stimulation of the human optic nerve. Proceedings of the 3rd Conference of the International Functional Electrical Stimulation Society (D. Popoviç, editor), Sendai, Japan, August 23-27, 1999, in press.

[13] Schmidt, E. M., Bak, M. J., Hambrecht, F. T., Kufta, C. V., O'Rourke, D. K., and Vallabhanath, P.: Feasibility of a visual Prosthesis for the blind based on intracortical microstimulation of the visual cortex. Brain 119: 507-522, 1996.

[14] Hambrecht, F. T.: Visual prostheses based on direct interfaces with the visual system. In: Bailliere's Clinical Neurology Vol.4 #1, G. S. Brindley and D. N. Rushton eds., Tindall, London, 1995.

[15]Bent AF, Sand, PK, Ostergard, DR, Brubaker, L. (1993) Transvaginal electrical stimulation in the treatment of genuine stress incontinence and detrusor instability Int Urogynecol J . 14:9-13.

[16] JL Buller, GW Cundiff, KA Noel, KS Leffler, JA VanRooyen, RM Ellerkman*, and AE Bent, "RF BION™: An injectable microstimulator for the treatment of overactive bladder disorders in adult females". American Urogynecologic Society (AUGS), Chicago 2001

[17] Shealy CN, Mortimer JT, Reswick JB. Electrical inhibition of pain by stimulation of the dorsal columns: preliminary clinical report. Anesth Analg 1967;46:489-91.

[18] Benabid et al. Chronic electrical stimulation of the ventralis intermedius nucleus of the thalamus as a treatment of movement disorders. *J Neurosurg* 1996; 84:203-14.

[19] Starr et al. Ablative surgery and deep brain stimulation for Parkinson's disease. *Neurosurgery* 1998; 43:989-1015.

[20] Minimed Inc. Northridge, California

[21] J. Parramon, P. Doguet, D. Marin, M. Verleyssen, R. Muñoz, L. Leija, E. Valderrama, "ASIC-based batteryless implantable telemetry microsystem for recording purposes", 19th International conference of the IEEE Engineering in medicine and biology society- EMBS'97, Chicago (USA) Oct 97

[22] O. Scholz, J. Parramon, J.-U. Meyer, E. Valderrama, "The design of an implantable telemetric device for the use in neural prostheses", XIV International Symposium on Biotelemetry, Marburg (Germany), Apr.97

[23] I. Rincon, A. Garcia-Rozo et al. "Telemetric monitoring of left ventricular pressure in a canine model of acute normovolemic hemodilution", ASAIO journal 44(2):84A, 1998.

[24] J. Parramon, B. D. Pendley, C. Rowan and M. R. Neuman , "An Integrated Sensor-Memory-Telemetry System", XV International Symposium on Biotelemetry, Alaska 1999

[25] D. Marín, O. Scholz, J. Parramon, T. Osés, J. Meyer, E. Valderrama. "Fast prototyping of implantable systems for stimulation and recording based on a bi-directional and rf-powered telemetry integrated circuit". 6th Vienna International Workshop on Functional Electrostimulation (IFESS'98). Proceedings. September. 1998, Vienna (Austria), pp. 81-84

CHAPTER TWO

TRANSCUTANEOUS POWER TRANSMISSION

2.1 INTRODUCTION

Any kind of device (electronic, mechanic, etc..) needs energy to become functional. So a concern for any system engineer is to be sure that power will be always there when required. In many easy-to-supply devices the problem related to power is essentially associated to cost. But in the micro implant world the problem of power goes beyond economics and becomes something essential in terms of functionality. Due to the usual small amount of energy available (small batteries) the way the engineer manages power becomes a key point in this industry. One of the focuses of this dissertation is to try finding paths to improve this parameter, what at the end means to increase the expected life-time of the device, and thus improving the life-quality of the subject carrying the implant.

The most common approach to provide energy to the implant is to use an *energy-container*, typically an electrochemical "deposit" like batteries. Due to the push in needs of the industry (specially in the portable communication systems sector), improvements in energy density and miniaturization have been accomplished. The new generation of primary Lithium cells [1] is a good example of that. Despite of these improvements there is still a long way to go. Other energy-container-like devices seem to be a promising future trend, especially with the new thin-film super-capacitors [2].

The above solution has a clear problem: as the energy source is embedded, once exhausted an explantation is mandatory to provide new energy. So the only chance we have to avoid surgical procedure is using an external source to deliver wireless energy in

order to (1) recharge the implanted batteries (using secondary batteries like Li-ion [3]) or (2) provide on-line power to the system. The latter refers to electromagnetic powering (EMP) of the system, which includes two main options: (1) RF going from a few kHz to few Mhz or (2) infrared up to light.

The first one has been widely proved as useful [4], thus permitting a reasonably easy development, especially when power needs are high (above 10mW). The infrared option has its own chances. Main interest of this approach is the small size of the implant that can be achieved, due to the use of photo diodes despite coils as receivers. But the power efficiency is very poor [5], hence non-practical for many implant applications and only useful for low-power transference. A third and more unexplored way is to find the power source in the same body, like thermal [6] or kinetic energy. But again very small amounts of energy can be supplied which in most of the cases make this solution useless.

Clear constrains in power demand makes the RF option the most atractive. Main idea of RF power is the use of magnetic energy stored in an external coil. When another coil is placed in the surroundings a coupling between both coils appear, and through electromagnetic induction a certain amount of voltage in the secondary (internal coil) is transferred from the external-primary tank. To understand better the concept we could also use a capacitor rather than a coil (so switching the magnetic field by an electrical field), but the capacitance value would be very low (capacitance coupling would be much smaller than magnetic coupling) and the power transference consequently would also be very poor.

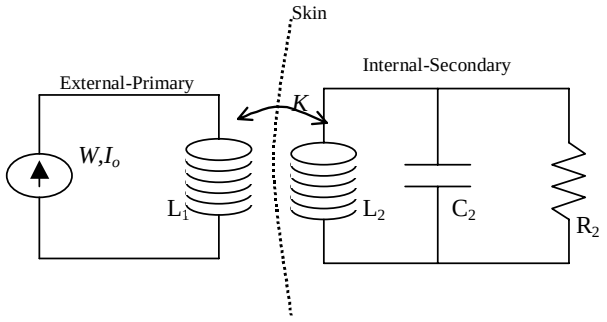

Figure 2-1. RF powering system

This technique as said, commonly referred as *RF Powering*, uses two coupled coils, the transmitter (primary) which is externally but close-to-the-skin positioned, and the receiving (secondary) which is a part of the implantable device. In this chapter, one of the first power systems using the RF technique that operates in the range of 10-20MHz is described. Previous works reported in the field used lower frequencies up to 1-2MHz [7]. Our approach makes compatible the power transfer with elevate communication bandwidth sharing the carrier for both purposes. In order to do so we had to push the frequency limits to regions were losses are difficult to avoid due to the intrinsic trade-off between power and frequency in any switching network. This chapter shows primarily the power system developed within the ITUBR project including a coil design and development, a custom-made chip receiver and an external transmitter

Within the RF-link analysis a novel mathematical analysis for very-low coupling factor is presented, which goes beyond current existing studies [8], and includes in the model the parasitic resistance of the coil, which proved to be very critical specially in the case where micro-coils are required. Finally two novel ideas concerning loop-control are proposed to further enhance the overall power efficiency of any RF link, especially relevant in our case were high frequencies yield to external transmitter losses.

2.2 ELECTROMAGNETIC COMPATIBILITY

This first part summarizes a very important issue concerning inductive power systems and its industrial way out: Electromagnetic compatibility (EMC). By definition is the ability of electronic devices or systems to operate in their intended environments without suffering or causing intolerable electromagnetic interference (EMI). For an active medical implant, EMC means that (1) it does not induce harmful effects to the patient's health and does not interfere with other nearby electronic equipment, and (2) it functions properly when exposed to the electromagnetic fields anticipated in the patient's environment. Epidemiological studies [9] suggested some connections between electromagnetic energy and biological disorders. In the RF powering approach, the

magnetic field generated by the external coil will interact with the patient's biological systems as well as with the implanted electronics. Despite the magnitude of the field in most cases is much smaller than other medical applications (like magnetic resonance imaging), it still produces measurable tissue heating [10] and some concern about safety regulations may certainly apply. An overview of the basic questions related to powering is presented next.

i) Electrical properties of tissue.

Most of the studies concerning the electrical properties of tissues were carried out during the 40's and 50's [11] [12]. Tissues are composed of cells filled primarily with fluids and encapsulated by thin membranes. The intracellular fluid consists of various salt ions, polar protein molecules, and polar water molecules. The extra-cellular fluid is similar to the intracellular fluid except that it has different proportions of the elements. When an AC signal is applied the oscillations of the free charges (ions) give rise to conduction currents (Eddy currents) and the rotation of dipole molecules at the frequency of the applied field effect displacement currents. This phenomenon is the basis for the biological reactions to electromagnetic fields. Power dissipation in tissue, resulting from ohmic losses associated with the conduction currents and dielectric losses associated with displacement currents, provide the energy necessary to induce most of the biological reactions to em fields (as we will analyze in part ii).

The electrical properties of any material and by extension any tissue can be summarized within the complex permittivity ε^*. Mathematically can be defined as:

$$\varepsilon^* = \varepsilon_0(\varepsilon' - j\varepsilon'')$$

where ε_0 is the permittivity in vacuum, ε' is the relative permittivity (dielectric constant) of the media, and ε'' is the loss factor. The effective conductivity of the media due to the sum of conduction current losses and dielectric losses is: $\sigma = \omega\varepsilon_0\varepsilon''$

and the loss tangent is: $tan\delta = \frac{\varepsilon'}{\varepsilon''} = \frac{\sigma}{\omega\varepsilon_0\varepsilon'}$ [13][14]

Next table (*Table 2.1*) shows some relevant constants of biological substances and its dependence on frequency. Ideally for a material without losses the effective conductivity should be zero, meaning that no conduction or displacement currents have been generated. For high water content tissue (like muscle and skin) the conductivity increases with frequency from 0.4mho/m at 1MHz to 10.3mho/m at 10GHz. This increase in effective conductivity means a decrease in depth of penetration, which is defined as the depth at which eddy current density has decreased to 1/e or about 37% of the surface density. In this case at 1MHz the em field penetrates 91.3cm and at 10GHz around 0.34cm.

For low water content tissue (like fat and bone) the same dependence with frequency appears. In this case tough, the absorption is smaller and the depth of penetration is larger compared to the high water content tissue.

Table 2-1. Electromagnetic properties for muscle and skin

Frequency (MHz)	**Wavelength in Air (cm)**	**Muscle, Skin, and Tissues with High Water Content**			
		Dielectric Constant ε_D	Conductivity ρ_L (mho/m)	Wavelength λ_L (cm)	Depth of Penetration (cm)
1	30000	2000	0.400	436	91.3
10	3000	160	0.625	118	21.6
27.12	1106	113	0.612	68.1	14.3
40.68	738	97.3	0.693	51.3	11.2
100	300	71.7	0.889	27	6.66
200	150	56.5	1.28	16.6	4.79
300	100	54	1.37	11.9	3.89
433	69.3	53	1.43	8.76	3.57
750	40	52	1.54	5.34	3.18
915	32.8	51	1.60	4.46	3.04
1500	20	49	1.77	2.81	2.42
2450	12.2	47	2.21	1.76	1.70
3000	10	46	2.26	1.45	1.61
5000	6	44	3.92	0.89	0.788
5800	5.17	43.3	4.73	0.775	0.720
8000	3.75	40	7.65	0.578	0.413
10000	3	39.9	10.3	0.464	0.343

Table 2.2. Electromagnetic properties for fat and bone

Frequency (MHz)	**Wavelength in Air (cm)**	**Fat, Bone, and Tissues with Low Water Content**			
		Dielectric Constant ε_D	Conductivity ρ_L (mho/m)	Wavelength λ_L (cm)	Depth of Penetration (cm)
1	30000				
10	3000				
27.12	1106	20	10.9-43.2	241	159
40.68	738	14.6	12.6-52.8	187	118
100	300	7.45	19.1-75.9	106	60.4
200	150	5.95	25.8-94.2	59.7	39.2
300	100	5.7	31.6-107	41	32.1
433	69.3	5.6	37.9-118	28.8	26.2
750	40	5.6	49.8-138	16.8	23
915	32.8	5.6	55.6-147	13.7	17.7
1500	20	5.6	70.8-171	8.41	13.9
2450	12.2	5.5	96.4-213	5.21	11.2
3000	10	5.5	110-234	4.25	9.74
5000	6	5.5	162-309	2.63	6.67
5800	5.17	5.05	186-338	2.29	5.24
8000	3.75	4.7	255-431	1.73	4.61
10000	3	4.5	324-549	1.41	3.39

ii) Biological effects.

Most of the literature concerning biological effects refers to low frequency (20-200Hz) or high frequency (200MHz-200GHz) ranges. So in our working range (1-30MHz) there is still a big lack of experimental data. There are two main effects to be considered: (1) thermophysiological, that is the capability of the thermoregulatory system in tolerating tissue heating due to e.m. field, and (2) athermal, where the field acts upon cellular structures.

In the first case the heating effects are not harmful as long as induced heat does not exceed the metabolic rate of an adult, which is about 1Watts/kg. In the second case it is well accepted from in-*vitro* and in-*vivo* studies that damage can be caused to the cell, mainly within the plasma membrane, by the EM fields [15]. Many additional effects (action potential disturbance, DNA synthesis alteration, etc.) are still unclear.

iii) Safety standards.

In 1966 a limit of safe exposure to electromagnetic radiation was established y the ANSI at $10mW/cm^2$, assuming that (1) thermally induced alterations were the only mechanism of biological effects and (2) by limiting the tissue heating by 1°C or less adverse bio-effects would be avoided. Recently the energy absorption in tissue was recognized as a much more realistic parameter than simply temperature rise. So a new magnitude, the SAR (Specific Absorption Rate) defined as the rate of energy dissipated per unit of mass was introduced. Mathematically we have $SAR=\sigma E^2/2\rho$ where σ is the electrical conductivity of the medium, E is the dissipated energy and ρ is the mass density of the medium.

ANSI developed a set of safety standards in 1982 revised by IEEE in 1991. Based in the most accepted RF exposure threshold to produce behavioral changes in animals (SAR=4W/Kg) the standard of safety was set with a security factor of 10. So SAR=0.4W/Kg for whole-body average. But local peaks of SAR can be tolerated far above this value. Specifically the spatial peak SAR value averaged over any 1g of tissue in cubic shape should not exceed 8W/Kg, except for ankles, wrists, hands and feet, where SAR averaged over any 10g of tissue should not exceed 20W/Kg. Moreover, any device radiating 7W or less with the radiator not within 2.5cm from the body it is considered safe and excluded from the above standards [16].

Exposures in excess of the standard may not be harmful, but are not recommended in absence of benefits. Other relevant conclusions from available literature include (1) damages from exposure to electromagnetic fields over separate periods are not cumulative, and (2) whole-body SAR is proportional to any partial body SAR when responding to the change in field strength .

iv) Safety concerns in Inductive Powered Implants.

The RF powering system considered here, where the maximum power radiated goes bellow 7W and the field generated is near field (decays very rapidly) makes the subject of implantation the only person whose safety should be studied. In most of the cases the 0.4W/Kg whole-body average is easily accomplished, so the concern is about local SAR peaks near the external coil.

v) Implant EMI protection

Obviously the electromagnetic field generated by the coils may well be a source of Electromagnetic Interference to (1) the external electronics surrounding the patient and to (2) the implanted electronics. In order to avoid the first problem the frequency chosen should be compatible with any radio-device near the implant and other instrumentation and if possible compatible with the FCC part 15 rules [17]. The second problem is usually solved by using metal encapsulation of the whole active implanted circuitry except (in the case of RF power) by the receiver coil that should be unshielded in order to receive energy.

As a matter of conclusion, we have seen that tissue absorption increases with frequency [see section **i)**]. So for the same amount of power required by the implant the transmitter will have to deliver more energy to compensate the loss. Depending on the package type, the case absorption may play a major role. The implant industry uses metallic casing for most of the long-term implants. And metal is a “electromagnetic hungry” material, that is, absorbs radiation very easily (and it heats up), especially for higher frequencies. So again the lower the frequency the safer and the more reliable the system. But there are other constrains that may point out towards higher frequencies, especially the communication bandwidth. Somehow a trade-off between all this parameters has to be reached in order to fulfill all the specs and build up a reliable and safe power transfer. The basic rule of thumb concerning RF power could be: *choose the*

lowest power transmission frequency compatible with the bandwidth constrains of the system and compliant with the FCC rules of maximum emitted radiation.

2.3 INDUCTIVE LINK

A RF power system includes three different elements: the inductive link (essentially a pair of coils), the implanted receiver and the external transmitter. This section focuses in the inductive link. Coil design as well as other link analysis will be investigated to obtain a reliable and efficient high-bandwidth RF powering system.

2.3.1 Basic concepts

An inductive link is basically a pair of coupled coils defining a transformer with a certain coupling factor. Physically the parameter to measure is the Mutual inductance between two coils (M). In a quasi-static approach were current changes are slow enough to consider the magnetic field in each instant identical to the one produced with a steady current, the electromotive force (EMF) induced in the secondary is proportional to the time-derivative of the primary current (*figure 2-2*). The constant of proportionality is M, the so-called Mutual Inductance [18]. Sometimes it is more useful the concept of coupling factor, defined as:

$$[2.1] \quad k = \frac{M}{\sqrt{L_p L_s}}$$

Where L_p is the primary (external) coil inductance and L_s is the secondary (internal) coil inductance (see *figure 2-1*).

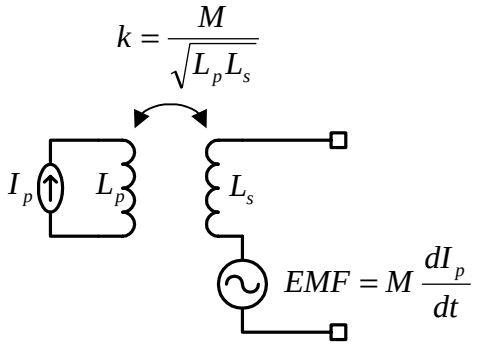

Figure 2-2. Basic transformer with secondary EMF

The k factor is generally more suitable as a design parameter because it does not depend on the number of coils (the M-dependence is canceled with the L_i dependence), thus making the analysis a little bit simpler.

In any case the amount of energy transferred depends greatly on this coupling what ultimately defines the power efficiency of the link and the tolerance of the system to lateral and angular misalignments.

2.3.2 Mutual inductance studies

In order to design properly the coils, a study concerning calculation of Mutual inductance (M) and coupling factor (k) must be done. Taking the definition of M [14] we have:

$$[2.2] \quad M = \frac{\mu_0}{4\pi} \oint\oint \frac{dl_1 \cdot dl_2}{r_{12}}$$

The mutual inductance of two circular air-cored loops (μ_r=1) whose axes are parallel (radii *a* and *b*, coil distance *d*) and with no misalignment can be expressed in a single integral [19][20]:

$$[2.3] \quad M(a,b,d) = \mu_0 \sqrt{ab}\, G(k) \quad where \quad k \equiv \sqrt{\frac{4ab}{(a+b)^2 + d^2}} \quad G(r) \equiv (\frac{2}{r} - r)K(r) - \frac{2}{r}R(r)$$

Where K(k) and E(k) are the complete elliptic integrals of the first and second kind respectively. This expression assumes a wire radius much smaller than both coil radius (*a* and *b*). See figure 2-3.

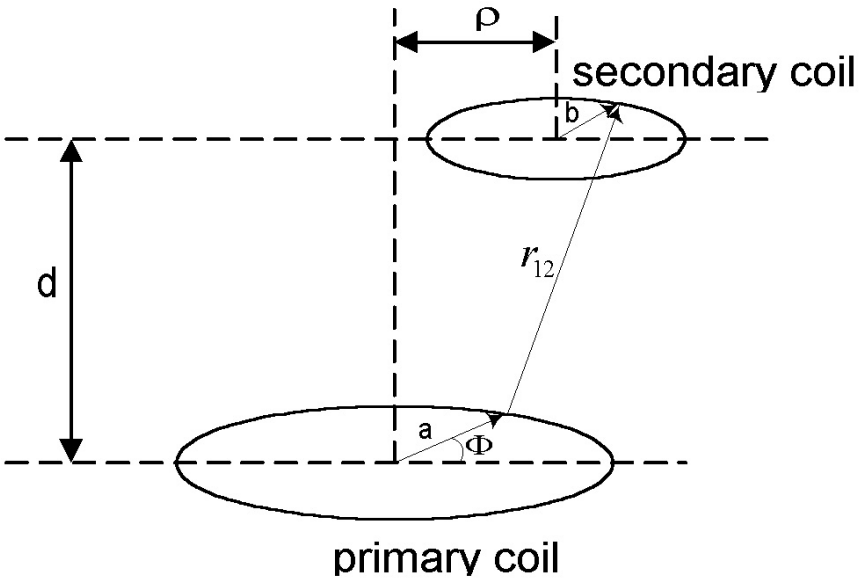

Figure 2-3. Coil to coil positioning with lateral misalignment

In case we have a lateral misalignment ρ (defined as the distance between the axes of both coils as seen in *figure 2-3*) we define the following parameters:

$$b_L \equiv \sqrt{b^2 + \rho^2 + 2\rho b\cos\phi} \qquad tan\beta \equiv \frac{\rho sin\phi}{b + \rho\cos\phi}$$

Then the mutual inductance will become:

[2.4] $$M = \frac{\mu_0 ab}{2\pi}\oint \frac{\cos\beta}{\sqrt{ab_L}} G(r)d\phi \qquad where \qquad r \equiv \sqrt{\frac{4ab_L}{(a+b_L)^2 + d^2}}$$

In case of ρ different to zero it is impossible to integrate exactly, so we must go towards a numerical integration. The formula [2.4] only refers to single-turn coils. In order to calculate mutual inductance for multi-turn coils we used a simplified approach. The approach used to calculate the mutual inductance between two coils separated a distance d, with a certain length (l_1 and l_2), number of turns (N_1 and N_2) and radii (a and b) is as follows:

$$[2.5] \qquad M = M_{sigle-loop}[a,b,d^{'}]* N_1 * N_2 \ \ where \ d^{'} = d + \frac{l_1}{2} + \frac{l_2}{2}$$

Basically this approximation gives accurate results as long as the distance between coils is much larger than the length of the two coils. Next graphic (*Figure 2.4*) shows a comparison between the theoretical values obtained once solved numerically[1] the integral [2.4] (with the approximation [2.5]) and the experimental values obtained in the lab, in a non-misalignment case.

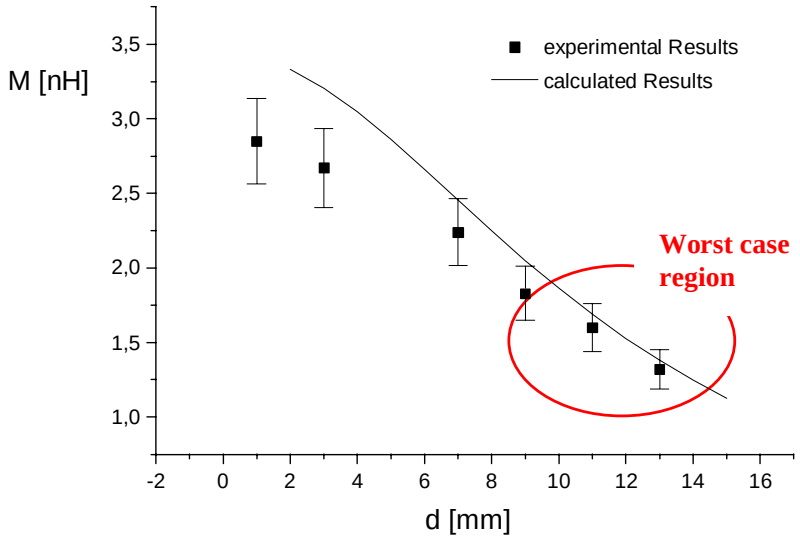

Figure 2-4. Mutual inductance experiments

The error of the theoretical approach, which considers planar coils at an additional distance of the average coil length increases as the distance between the coils decreases. In the area of our interest (from 5mm to 12mm) this approach has a maximum error of 21% at 5mm decreasing down to 6% at 12mm. The case with misalignment was also verified experimentally with similar results showing greater accuracy at larger distances. So basically we have proved that the calculation method that will be used extensively

[1] The numerical calculations were performed with the software Mathematica™.

when designing the coils is reasonably accurate in the operating range, especially in the upper distance range (around 1 cm). This is very important because that region defines the worst-case scenario of power transfer.

2.3.3 Coil development

The methodology used to design the coils is based in theoretical calculations of Mutual Inductance using the formulas presented above. Throughout this analysis optimum coil geometry is obtained. And once determined the optimum geometry the coils have been fabricated and characterized.

2.3.3.1 Coil Design

In order to achieve a good efficiency and to maintain a high tolerance to misalignments, the diameter of the inner coil should be as big as possible. In our case, a diameter of 10mm was chosen constrained by the implant size. Next, with a given operating distance and tolerance field, the diameter of the external coil was determined. As depicted in *Figure 2-5*, there is a maximum of mutual inductance versus external coil diameter for each operating distance. By using a small coil diameter, higher M should be expected for small distances. The general rule is that for small geometry the magnetic density can achieve larger values for close distances, but also decays faster, and therefore its variation with misalignment is much lager (see *figure 2-6*). So there is a trade-off between peak values and misalignment tolerance. Our range of operation, defined by the medical staff, lies between d=5mm, ρ=0 and d=12mm, ρ=12mm with a nominal operating distance of 8mm. Comparing *figures 2-5* and *2-6* we see that for the nominal distance (d=8mm) we have a M-peak around D1(external diameter) of 24mm. But the misalignment in the worst case is not that good. A compromise to select the diameter was taken with a final value of external diameter of 30mm. The M-value is fairly close to the peak for a nominal 8mm distance. And the misalignment figures are much better, with almost no change in M all over the working range. So a diameter ratio of 3 between the external and the internal coil will be used.

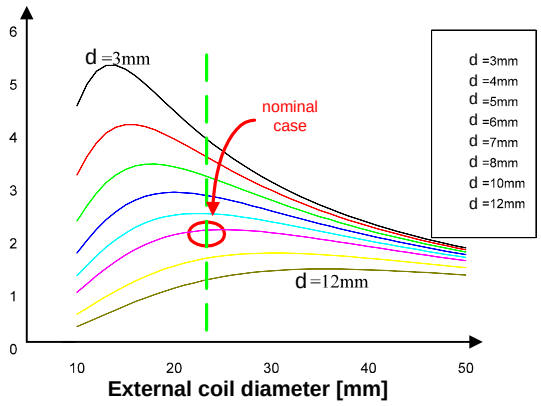

Figure 2.5. M(Y-axis) vs external coil diameter D_1 (D2=10mm)

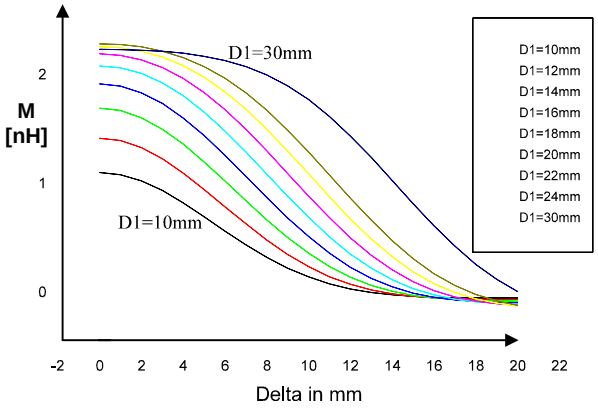

Figure 2.6. M(Y-axis) vs lateral misalignment Delta; d=8mm

In contrast to the mutual inductance, the coupling factor is independent of the number of turns and only depends on geometry. This makes the value interesting for general studies.

Through calculations, it is possible to find the best and the worst case coupling k for this particular case (though disregarding angular displacements):

$M_{min} = 0{,}929nH \Rightarrow k_{min} = 0{,}032$ @ d=12mm, ρ=12mm

$M_{max} = 2{,}954nH \Rightarrow k_{max} = 0{,}1$ @ d=5mm, ρ=7mm

Another possibility to optimize the coil design would be to try to work near the critical coupling [21]. The concept of critical coupling is essentially the following: for larger distances (as showed in detail in 2.3.4 [2-8]) the power transfer increases monotonously with M or k (as the intuition would say) but at very small distances (high M) the second order effect of the Mutual Inductance (reflection from the secondary to the primary) may have a bigger negative contribution than the first order effect (linear electromotive force proportional to M), thus defining a certain M-region where the power transfer has a maximum. Therefore near the maximum there is a region of very small first order variations. The problem is that the coupling in that region describes a fairly sharp

high-Q shape, thus only small variations of k (or M) can be accommodated. Unfortunately looking at the wide range of possible variation of the M (or k) for our application (from 0.929nH to 2.954nH) due to the distance and lateral misalignment variations, the critical coupling approach is not practical.

2.3.3.2 Coil Fabrication

Planar geometry air-cored coils of different size and inductance values have been fabricated with a reasonable capability of prediction. Post characterization of coils was achieved using a 40MHz impedance meter. Main parameters of a coil are L (self-inductance), Q (quality factor) and f_r (self-resonance). For the experiments on energy transmission, the coils described in table 2-2 have been used.

Table 2-2. Coil characterization

	∅ [mm]	Turns	Wire∅ [mm]	*@ 1MHz*		*@ 10MHz*		
				L[µH]	Q	L[µH]	Q	fR[MHz]
External	30	14	0,355	8,56	57	10,5	101	22,4
Internal	8	14	0,25	2,34	23	2,48	60	32,8

2.3.4 Very-low coupling analytical study

A particular case of interest, and yet fairly unexplored, is when the coupling factor is very small [22][23]. This is the case of any device powered by RF with a very small size (transponder business or injectable devices). Moreover a small coil not only implies low coupling but generally also poor quality factors. Although the CNM-ITUBR application does not necessarily implies extremely small coupling factor, a new theoretical analysis of this particular case has been performed extending the current theoretical studies, adding to the equations the impact of the parasitic coil resistance of the receiver coil. To do so a Matlab™ program has been developed as a tool that helps significantly the RF-link designer, compared with standard Spice simulations tools.

Next picture shows a typical Voltage-in Voltage-out (Serial-in Parallel-out) link configuration.

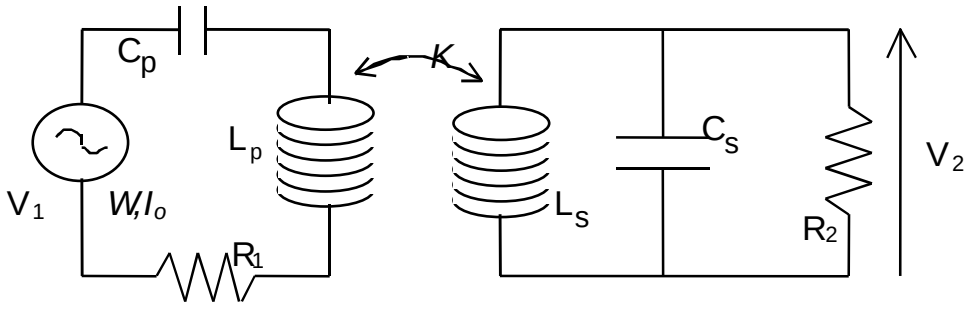

Figure 2-7. Voltage-in Voltage-out RF link

Essentially the best efficiency occurs when the output impedance of the primary source matches with the network. It has been shown [24] that the voltage gain transfer function can be found us:

$$[2.6] \quad \frac{V_2}{V_1} = \frac{M}{L_1} \frac{1}{k^2 + \frac{L_2 R_1}{L_1 R_2}}$$

For a fixed secondary load the power increases with the voltage. So in order to optimize the power transfer one should basically go to the prior mentioned critical coupling point kc, defined by the condition [2.7]:

$$[2.7] \quad \frac{\partial}{\partial k}\left(\frac{V_2}{V_1}\right)_{k=k_c} = 0 \qquad [2.8] \quad \frac{V_2}{V_1} = k\sqrt{\frac{L_1}{L_2}}\frac{R_2}{R_1}$$

In the case of extremely small coupling factor ($k^2<<1$) the second order effects of the coupling factor are neglected, so the gain transfer is given by [2.8]. This formula basically tells that the higher the coupling factor and the smaller the secondary inductance the better the efficiency, for a constant load and an optimized primary circuit. This is not the case in reality when you must include in the model the losses of the receiver coil.

A calculation method using Maxwell equations to evaluate the power transfer is presented next. The transformer within the Voltage-in/Voltage-out configuration (*Figure 2.7*) can be modeled as follows.

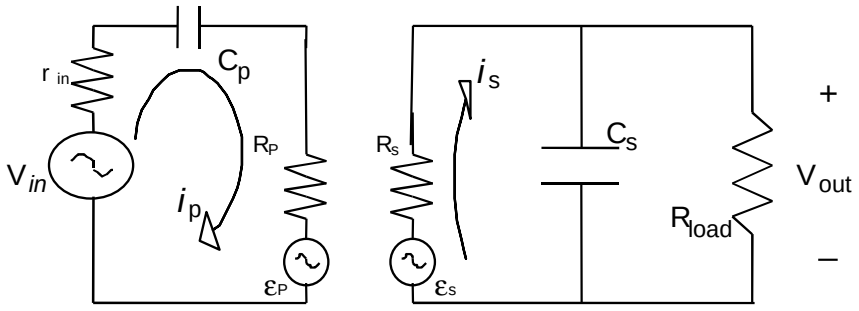

Figure 2.8. Equivalent model of Voltage-in/Voltage-out Link

Using the third Maxwell equation in the quasi-static approach the next set of equations follows:

[2.9] $$\varepsilon_p = k\sqrt{L_p L_s}\frac{di_s}{dt} - L_p\frac{di_p}{dt}$$

[2.10] $$\varepsilon_s = k\sqrt{L_p L_s}\frac{di_p}{dt} - L_s\frac{di_s}{dt}$$

And solving the circuit network:

[2.11] $$V_{in} + \varepsilon_p = i_p\left(R_p + r_{in} + \frac{1}{C_p s}\right)$$

[2.12] $$\varepsilon_s = i_s\left(R_s + \frac{R_{load}}{1 + R_{load}C_s s}\right)$$

Assuming that the inductance of the secondary coil towards the primary coil may be far weaker than the self-inductance of the primary coil (small coupling factor) we have:

[2.13] $$\frac{d\phi_{21}}{dt} = L_p\frac{di_p}{dt} << \frac{d\phi_{11}}{dt} = l\sqrt{L_p L_s}\frac{di_s}{dt}$$

Combining [2.9] plus [2.11] with the [2.13] first order approach and [2.10] plus [2.12] and solving the differential equation we finally obtain:

[2.14] $$\frac{V_{out}}{V_{in}} = \frac{M\omega}{R_p + r_{in}}\frac{\Theta}{(R_s + \Theta + L_s s)} \quad \textit{where,}$$

[2.15] $$\Theta \equiv \frac{R_{load}}{1 + R_{load}C_s s}$$

This is the Voltage Gain transfer function taking into account the non-ideal parameters of the coil (finite Q). It can be easily proved that for the case without parasitic resistance we recover the expression [2.8].

The theoretical effort has been basically carried out to decrease design time. Obviously you can go to the electric simulator, but if many parametrical sweeps are required the computation time grows too fast. A comparison between the analytical first-order method using Matlab and the exact Spice calculations was performed. The difference in design time is significant. Using HP workstation with Eldo™ simulator it took about 1 hour including real computation time plus design time to carried a set of parametric sweeps. Each data point in a Gain-transfer diagram was actually obtained by finding the peak-point of an AC analysis. As opposed to that, a simple Matlab™ program using the [2.14] equation can perform the analysis in about 10 seconds. Obviously the Eldo™ simulated results are more accurate, but with small coupling factor (bellow 0.02) the first-order approach proves to be very accurate (see *Figure 2-9*). First-order theoretical calculations computed with Matlab™ are the continuous line.

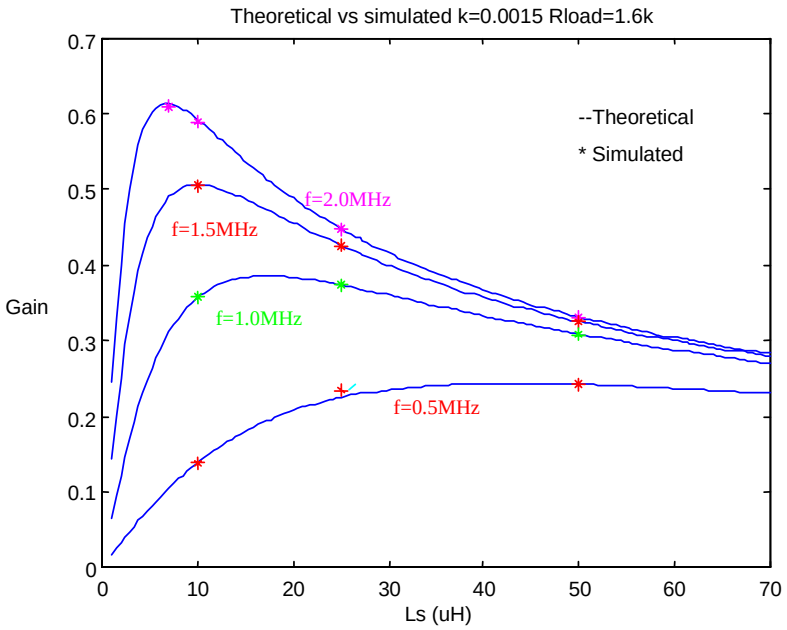

Figure 2-9. Non-approximate simulations versus first-order analytical approach

This theoretical approach using first order approximation is also usefull to have a better comprehension of the link itself, giving a simple way of understanding how each variable impacts the overall transfer. For instance within the k<<1 approach there is no critical coupling because the higher the Mutual Inductance the better the gain. Also it can be seen that for any given frequency there is a critical secondary inductance ($L_{s,crit}$) where the Gain is maximum.

2.4 INTERNAL POWER RECEIVER

This section describes the design of the implanted RF Power receiver, developed in the framework of the CNM-ITUBR project. In order to pick up the incoming RF energy a special circuit was used to handle high input voltages above 20 volts. The front-end receiver was a tuned LC tank matched to the transmitter frequency. Thus depending on the coupling factor (which varies with distance, orientation, etc.. see section 2.3.2) a certain voltage signal is induced. Amplitude ranges can go up to 60V peak-to-peak, if strong coupling and very efficient power transmitter applies. Figure *2-10* shows the energy-receiver circuit implemented.

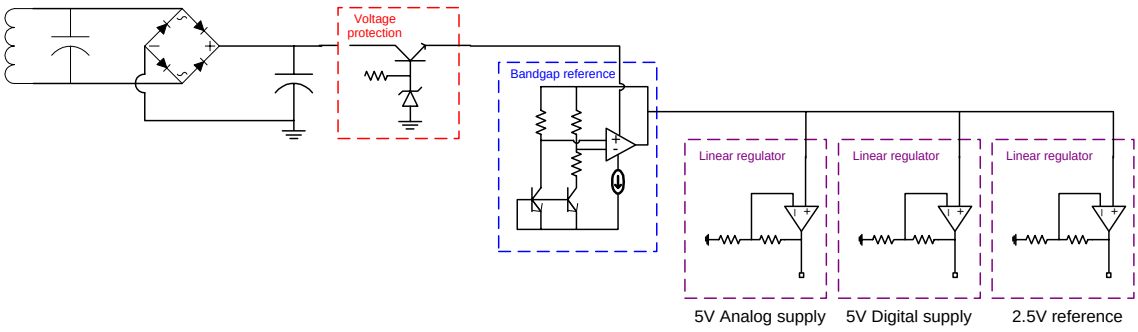

Figure 2-10. Energy-receiver circuit

Once induced the signal in the terminals of the receiving coil, the AC signal is full-rectified using a Schottky-diode bridge, hence defining two output nodes: ground and

rectified voltage. In the next stage the incoming voltage is pre-regulated using a characterized zener diode and a NPN transistor which at the same time is acting as an input voltage protector of 11.7V threshold. Through the use of a double BandGap voltage reference, a final dual 5V supply lines (analog and digital) plus a 2.5V reference is obtained using three output buffers with resistor-ratio programmed gain stages (series regulator).

2.4.1 Integration

In this section, some of the key elements in the design of the energy front-end in terms of chip design are presented.

i) *Technology*: The concern of dealing with large input voltages was the major constrain for choosing a certain IC technology. Through Europractice program the best solution was to use the ALCATEL-MIETEC 2.4um CMOS process with a certain changes in the fabrication steps in order to include high voltage gates (up to 50V) and also bipolar transistors. The process is named HBIMOS.

ii) *LC front-end*: The 5-20MHz range of the RF powering did not allow integration of the coil either the capacitance. Typical values of these integrated elements are bellow 1 μH with very low Qs for the coils and hundreds of picofarads for the capacitors. Hand-made air coils (section 2.3.3.2) and commercial trimming capacitors were used to match the frequency.

iii) *Diode bridge*: A great concern in power efficiency was given to the full-wave rectifier, because a bad switch time in the diode may results in very big power loses due to large dropping voltage in the diodes terminals. A first trial intending to integrate the diodes into the HBIMOS technology [25] showed very poor switching times, thus we had no other chance than using a special high-speed high-voltage Schottky diodes for the rectifier bridge.

iv) High Voltage regulator: A nice feature of the chosen HBIMOS technology was to provide a 11.7V nominal zener diode. Taking profit of this fact a very well protected to high voltages 5V line regulator was designed and used in several chips.

Although simplified, figure 2-11 depicts the essential elements of the voltage regulator.

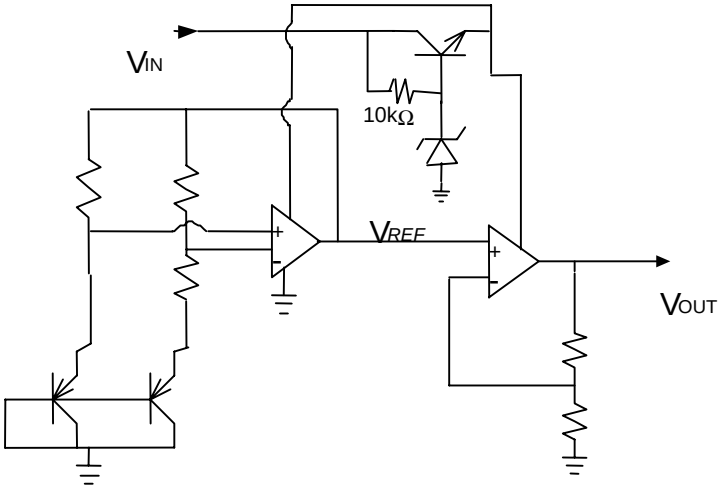

Figure 2-11. Simplified voltage regulator schematic

The pre-rectified voltage is the emitter of a bipolar transistor with a zener diode in its base. A BE feed-back resistor (10kΩ integrated in high poly resistance) assured proper biasing of the zener. So this structure assured a voltage protection and pre-regulation if voltages higher than 12V were induced (the zener diode voltage drop is locked to 11.7V, and the collector voltage goes Vbe higher). Next step was a 5V regulator using a well defined and temperature insensitive (zero temperature coefficient) voltage reference provided by a bandgap cell. A non-inverting high power-supply-rejection buffer stage with the exact gain to deliver 5V was placed as the output of the regulator. In addition to that a 2.5V reference was also included. This was used in several parts of the analog front-end as well as to set the electrode biasing (defining the input common mode).

Table 2.3 shows a set of energy-receiver voltage regulator specifications.

Table 2-3. Simulated voltage regulator parameters

DC input range	Load sensibility	DC sensibility	Power@7V
7 to 20 V	<1mV/kΩ	<0.3mV/V	1.08mW©7V

2.4.2 Results

Once translated to silicon the on-chip receiver had an overall area of 880x800 μm^2, including the zener-based pre-regulator, the bandgap voltage reference, the current generator and three buffered voltage lines each including a low PSRR OpAmp. Figure 2-12 shows a microphotograph of the circuit:

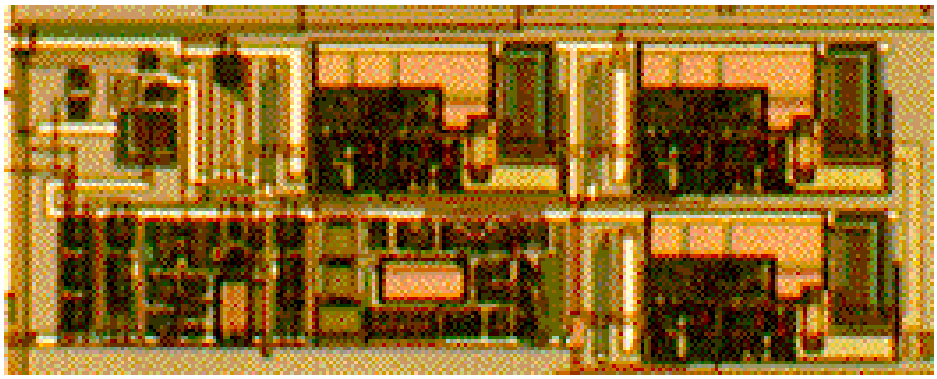

Figure 2-12. On-chip energy receiver microphotograph (HBIMOS technology)

Table 2-4 shows the experimental data of the supply line provided by the energy receiver integrated within the CNM-ITUBR system.

Table 2-4. Experimental results of the voltage regulator

DC input range	Load sensibility	DC sensibility	Power@7V
7.1 to 20 V	<1.6mV/kΩ	<0.9mV/V	1.12mW©7V

Figure 2-13 shows the regulated output as a function of the induced voltage.

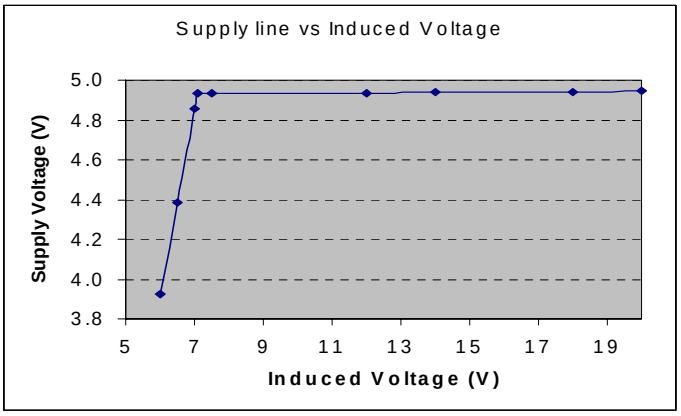

Figure 2-13. Supply line versus induced voltage

We see a fairly stable voltage supply beyond 7.1V of input voltage with a nominal output voltage around 4.94V. Bellow that level the regulator starts to fall down, resulting in a forward drop voltage around 2.1V. The supply variation due to input voltage changes is about 0.9mV/V with a quiescent consumption of 1.12mW at 7.1V.

2.5 EXTERNAL POWER TRANSMITTER

Since the early steps of the Transcutaneous Link development an important effort was devoted to the non-implanted part of the system. The major challenge was to design a RF transmitter able to power the implant and at the same time capable to communicate at a high data rate keeping power efficiencies at reasonable levels. As far as this chapter concerns we will only deal with the energy transmission. The critical element of the external transmitter is the circuit to drive the coil. There are many types of amplifiers that may be suitable. Among them Class-D and Class-E with both theoretical 100% of efficiency (only ideal switches) are very suitable candidates. The topology chosen is Class-E. The major advantage of this topology versus other types (like class-D or class-C) is essentially the easy inclusion of the parasitic drain-source capacitance of the switch transistor into the design optimization, because a tuning capacitor across the transistor is

required. Another reason, now dealing with the communication itself, is the fact that a simple supply modulation results directly in amplitude modulation of the coil current [20].

2.5.1 Class-E design

The class-E amplifier was introduced in 1975 by Sokal and Sokal [26]. It is a very interesting structure when high power efficiency is a primary concern. A simple class-E driver consists of a transistor with a shunt capacitor, a RF choke inductor to provide a constant current from the power supply and a series RLC load network which is tuned to a certain frequency. The basic scheme is shown in *figure 2-14*. In this scheme the inductance of the RLC series circuit will be the transmitting antenna in the telemetry system. This configuration is a multi-frequency load network because there are two relevant resonance frequencies: the series resonance of the RLC network and the parallel resonance of the total shunt capacitance (C_{shunt} plus the parasitic drain-source capacitance of the transistor (C_{ds})) together with the RLC network.

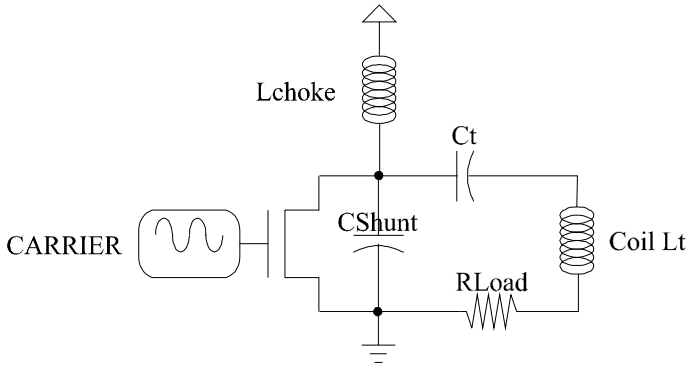

Figure 2-14. Class-E coil driver

The transistor is driven by a periodic signal acting as a switch. The transistor can be a FET or a BJT. In what follows we use a MOSFET. The drain-source voltage is determined by the transistor when it is ON (very close to ground) and by the transient response of the load network when it is OFF. As we will show in the next paragraph we take advantage of this fact to reduce the switching losses in the transistor.

The high efficiency of class-E amplifiers is achieved by reducing the transistor switching losses in the following ways:

i) The transistor is turned-on when the drain voltage has come back to zero, reducing the turn-on loss.

ii) The slope of the drain voltage is also zero at the time of turn-on, which allows for slight detuning without loosing efficiency.

The above two conditions define the optimum point of operation or *class-E point* where the maximum efficiency and maximum output power in class-E drivers is reached. The class-E operation point of the amplifier was analyzed by Raab [27], giving a simple set of equations for a 50% duty cycle of the transistor operation (D=0.5, see *Table 2-5*). A more complete analysis, also for idealized operation, is presented by Kazimierczuk in [28]. In this article the design of class E drivers working in the optimum point operation is shown for different switch duty cycle (D) and quality factor of the RLC network (Q). However, to simplify the generation of the carrier frequency, we will consider 50% switch duty cycle, as is the case in most class-E drivers.

The main assumptions taken are: (1) the current through the RF choke is constant; (2) the quality factor of the RLC series circuit is high enough to presume the output current (through the RLC circuit) is sinusoidal; (3) the transistor has zero saturation voltage (in case we consider a BJT), zero on-resistance and infinite off-resistance and (4) the total shunt capacitance is independent of the drain voltage (i.e. the influence of the variation of the parasitic capacitances with the drain voltage are not considered).

Table 2-5. Class-E driver optimum point equations

Parameter definition	Equations for D=0.5	Eq. Nº
R_T = total load resistance. R_{Scoil} = coil resistance at switching frequency f, $\omega=2\pi f$. R_e = series resistance reflected to the class E driver from the resistive load across the receiver coil.	$R_T = R_{LOAD} + R_{Scoil} + R_e$	(1)
C_{TSHUNT} = Total shunt capacitance ($C_{SHUNT}+C_{DS}$)	$C_{TSHUNT} = \frac{1}{5{,}4466 \cdot \omega R_T}$	(2)
X = series reactance at f frequency.	$X = \omega L_T - \frac{1}{\omega C_T} = 1{,}1525 \cdot R_T$	(3)
V_{DS_PEAK} = maximum amplitude in the drain to source voltage. I_{DS_PEAK} = maximum amplitude in the drain to source current.	$V_{DS\_PEAK} = 3{,}56 \cdot V_{CC}$ $I_{DS\_PEAK} = 2{,}84 \cdot I_{CC}$	(4) (5)
V_t = amplitude of the AC signal through the transmitter inductor L_T.	$V_t = 1{,}074 \cdot V_{CC}$	(6)
R_{DC} = equivalent resistance that the amplifier shows to the power supply V_{CC}.	$R_{DC} = 1.7337 \cdot R_T$	(7)
P_{IN}= input power	$P_{IN} = \frac{V_{cc}^2}{R_{DC}}$	(8)
$\lvert i_C \rvert$ = amplitude of the AC current though R_T.	$\lvert i_C \rvert = \frac{1{,}074 \cdot V_{CC}}{R_T}$	(9)

These assumptions are acceptable for low frequencies (less than 5MHz) where the turn-on and turn-off time of the transistor are negligible. At higher frequencies, the values of the components become only an approximation and they have to be adjusted to achieve the optimum operating point. From these equations the main components values and characteristics (e.g. the maximum ratings of the transistor) can be derived.

Using the result obtained in section 2.3.3.1 a ration of 3 between external and internal coil was chosen (minimizing lateral misalignment impact), with an external coil diameter of 30mm. With that dimension a coplanar 1µH coil with a resistance of 494mΩ

at 10MHz was used as an input of the design. Hence following the Kazimierczuk equations the table 2-6 was obtained.

Table 2-6. Class-E component values vs Quality factor

Kazimierczuk Table				**Component values calculation**				
Qt	**ω*Lt/R**	**ω*R*Ct**	**ω*R*C_{SH}**	**R (Ω)**	**Ct (pF)**	**C_{SH} (pF)**	**f_{RLC} (MHz)**	**f_{off} (MHz)**
1	2,104	2,104	0,2204	29,86	1121,33	117,46	4,75	15,43
2	2,85	0,7124	0,219	22,05	514,29	158,10	7,02	14,47
3	3,75	0,4166	0,215	16,76	395,72	204,23	8,00	13,71
5	5,673	0,2269	0,2067	11,08	326,05	297,03	8,81	12,76
7	7,642	0,156	0,2017	8,22	301,98	390,44	9,16	12,19
10	10,62	0,1062	0,1971	5,92	285,69	530,21	9,42	11,68
15	15,61	0,06936	0,1931	4,03	274,25	763,53	9,61	11,20
20	20,6	0,05149	0,1909	3,05	268,68	996,12	9,71	10,94
100	100,58	0,01006	0,1851	0,62	256,30	4715,83	9,94	10,20

Finally a Quality Factor (Q_t) of 5 was chosen because although it provides less output power for the same power supply voltage, the variations in the coupling with the receiver do not lead to a considerable decrease of the efficiency and at the same time is low enough to allow high-bandwidth modulation. The choke inductance should guarantee that the supply current of the class E amplifier stays approximately constant during the RF cycle. The relationship between its value and the switching frequency is usually defined by:

$$L_{CHOKE} > 3.5 \cdot \frac{R_T}{f_C}$$

The power switching transistor of the class-E driver is a N-channel Enhancement-Mode MOS VN66AFD transistor with 66V maximum drain source voltage, 1 A maximum DC current and 15 ns rise and fall time. The package of this transistor is a TO-220 that allow easy placement of a heat sink.

2.5.2 Results.

The measurements done on the class-E driver operating at 10MHz show transmitter efficiencies above 70%. In terms of overall power efficiency (transmitter + link + receiver) next table (*Table 2.7*) shows the results obtained at a fixed nominal distance (6mm) and with a 1.5kΩ load (emulating implant equivalent consumption).

Table 2-7. Overall Power efficiency

f_T (MHz)	V_{CC} (V)	I_{CC} (mA)	V(V) @ 1.5KΩ	Power to the load	Global Efficiency η_T
11	5	270	18	0.216W	16%
11	10	390	29	0.560W	14.3%

So transmitter efficiencies above 70% and global efficiencies of power transfer in the range of 15% were reached. Values that can be considered as pretty good due to the big constrain imposed by the high values of carrier frequencies if compared with former RF Powering systems developed.

In terms of distance of operation and misalignment sensibility figures 2-15 and 2-16 show the results obtained.

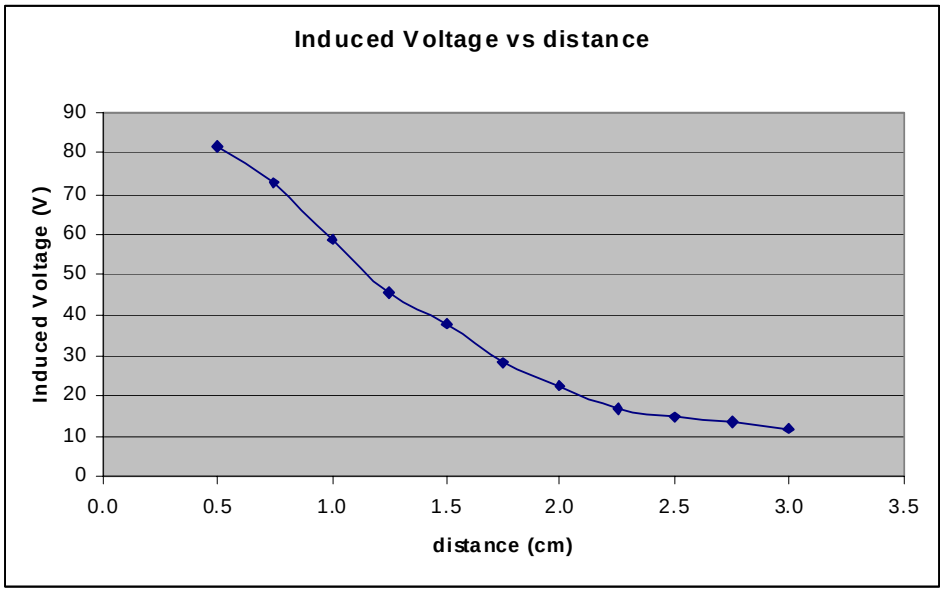

Figure 2-15. Induced Voltage versus distance

We see that for closer distances very large current can be achieved (up to 80V). Enough power was transferred for all distance range of operation (defined as 15mm). The minimum voltage to operate was around 7V, so with this system we could successfully transmit the required energy to a distance larger than 30mm.

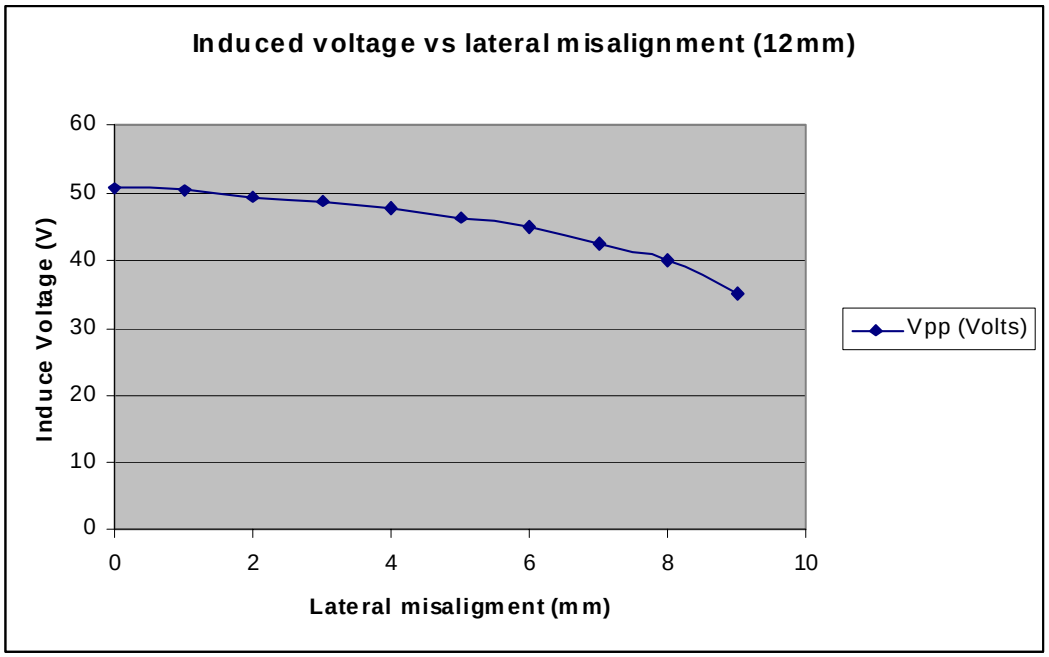

Figure 2-16. Induced Voltage versus lateral misalignment

Due to the 3:1 diameter ratio chosen the misalignment tolerance is fairly good. Even for a misalignment of the same magnitude of the implanted coil we have a voltage reduction of only about 20%.

The angular variation was also investigated. In that case we see a change in 18% of the induced voltage for a 15-degree angular misalignment at a distance of 17mm (see figure 2-17).

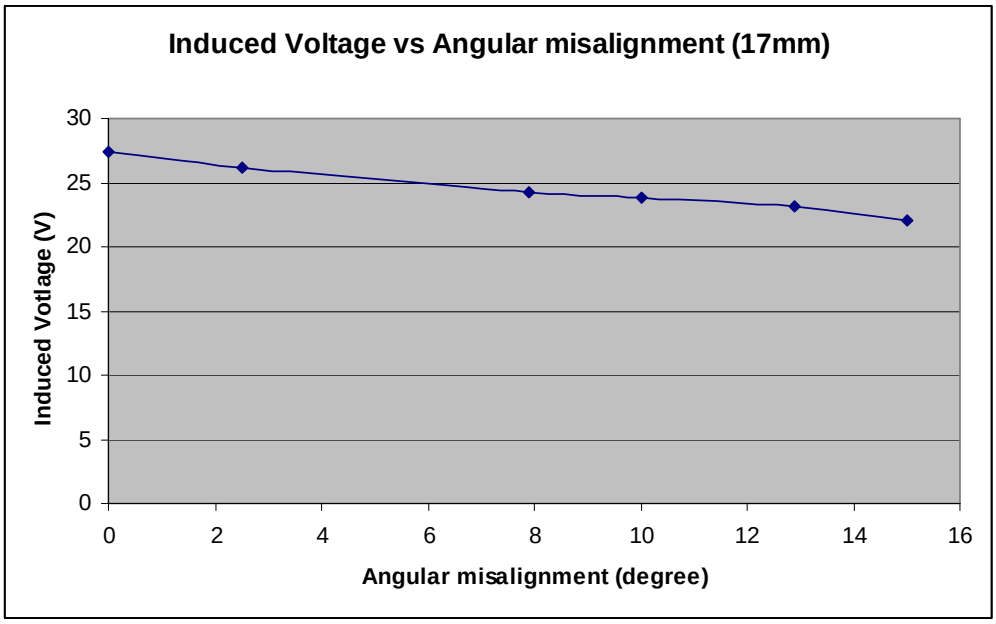

Figure 2-17. Induced Voltage versus angular misalignment

2.5.3 New design solutions to improve power transfer efficiency

Despite the driver efficiency achieved is rather good (around 70% see section 2.5.2), two new ideas to improve the overall link efficiency are presented.

2.5.3.1 Close-loop induced voltage control

This idea implies a close-loop control of the transferred voltage using the back-telemetry channel. Essentially a continuous monitoring of the induced voltage in the implant is sent back to the external unit that processes the information and reduces or increases the amount of energy transmitted as needed. As seen in figure 2-18.

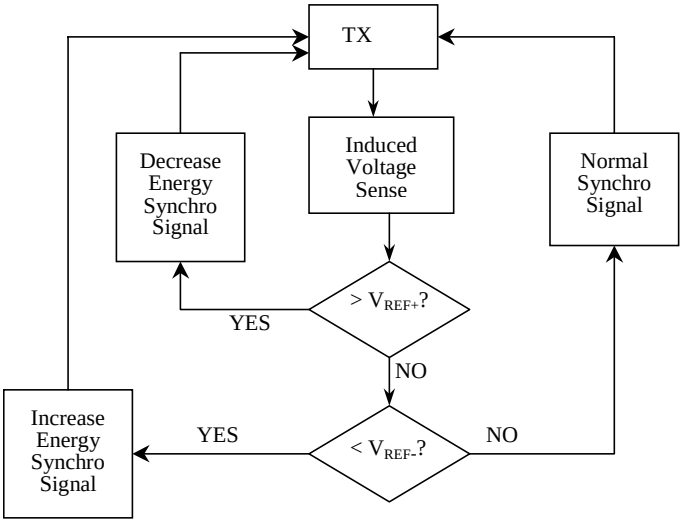

Figure 2-18. Close-loop induced voltage protocol

One major drawback of this technique is that requires a certain amount of bandwidth of the back channel. A solution to this problem has been proposed using a dedicated synchronization signal already required in the communication protocol (see chapter four). After defining a range of voltages of operation, each of the possible three states (above-range, below-range and in-range) codifies a different synchronization signal sent to the external unit. With a small increase of external circuit complexity the transmitter will know at any time if the implant is correctly powered, if its over-powered or if it is dangerously near an under-powered situation. In terms of design, a simple two-comparator scheme with resistor dividers was implemented as shown in figure 2-19.

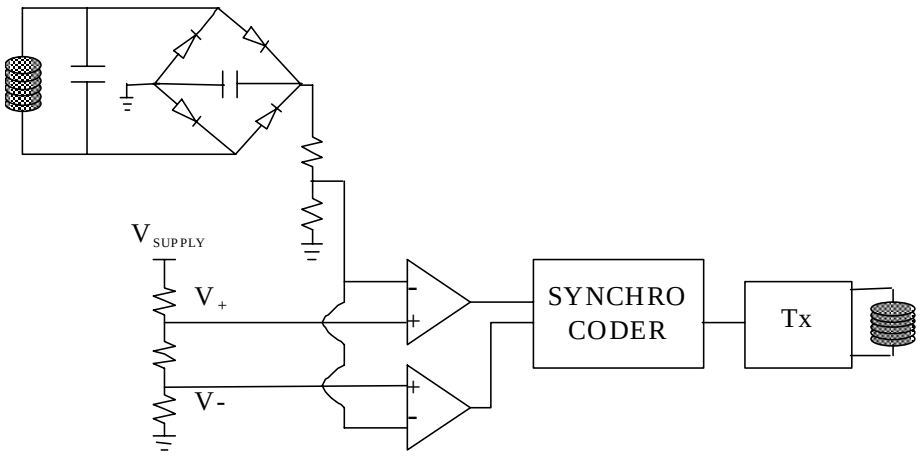

Figure 2-19. Close-loop control circuit

Two voltage references defining the upper and lower voltage range of operation are compared with the incoming previously divided induced voltage. The three states are codified as shown in table 2-8.

Table 2-8. 2-bit close-loop control

	Below-range	**In-range**	**Over-range**
Bit0	0	0	1
Bit1	1	0	0

Each of the three possible states is sent to the external controller through the back-telemetry channel. In order to not interfere with the standard communication protocol and also without wasting bandwidth. There is a dedicated hard-coded synchronization signal (used to robust the communication) for each of the three states.

This concept was introduced in the TIC chip (see chapter four, section 4.3) where a general purposed chip interface providing energy and data to any implant is described.

2.5.3.2 Class-E self-adaptation design

The class-E circuit can be optimized in different ways if stand-alone, that means if no influence of any reflected load. The major source of energy losses is due to the switching losses when slightly out of tuning. As we have already seen in section 2.5.1 Kazimierzcuk et al showed a way of optimize the Class-E for different range of frequencies and quality factors. Basically with the adequate inductance and capacitance values the switch may turn ON just when there is a zero voltage drop across the drain-source of the transistors (no energy stored in the series capacitance is lost). This approach has the problem that for a variable impedance network (that's the case of the transmitter when different coupling factors in the link may define different reflected impedances) you must change any of the passive elements up to reach again the optimum point. An active circuit to detect the right moment to turn-on the switch has been also presented in different papers [29] using a zero-crossing circuit controlling the gate-source voltage of the

switch. This idea works well and makes the class-E driver to operate with good efficiencies with variable loads. But there is no control on the exact amount of energy effectively transferred to the implant.

A novel power-adaptive system idea is presented, were through sensing the primary-coil current the transmitter can evaluate the coupling factor (k) knowing the secondary load as well as the rest of the network parameters (inductances and quality factors).

Different authors have investigated the capabilities of sensing the reflected impedance to achieve communication with the implant (see chapter three section 3.2.2.1). The solution proposed here goes beyond that and extracts real coupling factor information that will be used to optimize the power transfer link. As we see in *Figure 2-20* the reflected impedance is proportional to M^2 and inversely proportional to the secondary load.

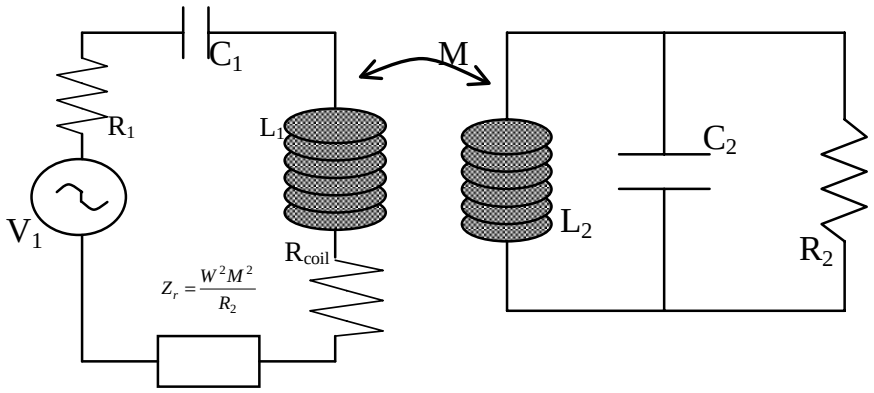

Figure 2-20. Reflected impedance sensor

In a low frequency range most of the reflected impedance is real. The relation between the primary current and the secondary parameters are as follows:

$$I_1 = \frac{V_1}{(R_s + R_{coil} + \frac{\omega^2 M^2}{R_{load}})}$$

Therefore if the inductances and quality factors of both primary and secondary coils are known and if the secondary load is also pre-defined, then the mutual inductance (M) and as a consequence the coupling factor (k) will be determined. This is the first step to the magnetic field regulation. Once the coupling is known, it is possible to calculate the exact magnetic field (primary current) required to meet the power requirements. Essentially the concept here described is very similar to the one presented in section 2.5.3.1. In the former section the information about the coupling (coded in the induced voltage) was sent back by telemetry means. In this section the method described do not require any back telemetry, what simplifies the implant design (even though increases the external controller complexity). Obviously this concept only can be used when reasonably high coupling factors apply (hence the reflected impedance is measurable). For low-coupling systems, the back-telemetry close-loop solution proposed earlier is still the only feasible solution.

2.6 REFERENCES

[1] Colin A. Vincent, Bruno Scrosati, "Modern Batteries, An introduction to electrochemical power sources", Butterworth-Heinemann find supercapacitor reference

[2] B.E. Conway, "Electrochemical supercapacitors", Kluwer Academic/Plenum publishers, New York

[3] Galina Dern, "Advances in Li-ion and Li-polymer: comparison of Li-ion Prismatics vs Polymers", Power'99, San Diego 1999

[4] J.C. Schuder et al., "High level electromagnetic energy transfer through a closed chestwall", IER Int. Conv. Rec., pt.9,vol 9, pp.119-126, 1961.

[5] D. Edell, "Chronically implantable neural information transducers", 18th Conference of the IEEE EMBS, Mini-Symposium on Neurotechnology session, Nov'96

[6] Applied Digital Solutions, "Miniaturized Thermoelectric Generator Powered by Body Heat"

[7] P. Troyk, M. Schwan, "Closed-loop class E transcutaneous power and data link for microimplants", IEEE Transactions on Biomedical Engineering, vol. 39, nº6, Jun'92

[8] T. Akin, K. Najafi, R. Bradley, "An implantable multichannel digital neural recording system for a micromachined sieve electrode", 8th conference on solid-state sensors and actuators, 51-54, June 95

[9] T.S. Perry, "Today's View of Magnetic Fields", IEEE Spectrum, vol. 31, No.12, pp. 14-23, 1994.

[10] E. Hochmair, “System optimization for improved accurancy in transcutaneous signal and power transmission”, IEEE transactions on biomedical engineering, vol. BME-31, nº2, Feb'84.

[11] J.M. Osepchuk (ed), Biological Effects of Electromagnetic Radiation. New Yor, NY: IEEE Press, 1983.

[12] H.P. Schwan, “Electrical Properties of Tissue and Cell Suspensions”, in J.H. Lawrence and C.A. Tobias (eds.), Biological and Medical Physics. New York, NY: Academic Press, 1957

[13] C.C. Johnson and A.W. Guy, “Nonionizing Electromagnetic Wave Effects in Biological Materials and Systems”, Proc. IEEE, vol.60, pp.692-18, 1972.

[14] H.P. Schwan, “Electrical Properties of Tissue and Cell Suspensions”, in J.H. Lawrence and C.A. Tobias (eds.), Biological and Medical Physics. New York, NY: .Academic Press, 1957

[15] S.F. Cleary, “Biological Effects of Radiofrequency Electromagnetic Fields”, in O. P. Gandhi (de.), Biological Effects and Medical Applications of Electromagnetic Energy. Englewood Cliffs, NJ: Prentice Hall, 1990.

[16] The IEEE Standard for Safety Levels with Respect to Human Exposure to Radio-Frequency Electromagnetic Field, 3 KHz to 300 GHz (IEEE C95.1-1991, Revision of ANSE C5.1-1982). New York, NY: IEEE Press, 1991.

[17] FCC rules and regulations , part 15

[18] “The Feynman Lectures on Physics”, Volume II, Electromagnetism and matter

[19] M. Soma, D. Galbraith, R. White, “Radio-frequency coils in implantable devices: misalgnment analysis and design procedure”, IEEE transactions on biomedical engineering, vol.BME-34,nº4,276-282, April 87

[20] C. Zierhofer, E. Hochmair, "Coil desing for improved power transfer efficiency in inductive links", 18th Conference of the IEEE EMBS, 5.8.2. Voice and neuroprosthetic augmentation session, Nov’96

[21] E. Hochmair, “System optimization for improved accurancy in transcutaneous signal and power transmission”, IEEE transactions on biomedical engineering, vol. BME-31, nº2, Feb'84.

[22] G.E. Loeb, C.J. Zamin and J.H.Schulman, “Injectable microstimulator for functional electrical stimulation”, Med.&Biol.Eng.&Comput., vol.29,pp.NS13-NS19, 1991.

[23] M. Nardin, K.Najafi, “A multichannel neuromuscular microstimulator with bi-directional telemetry”, 8th conference on solid-state sensors and actuators, 59-62, Jun’95

[24] T. Akin ,“An integrated telemetric multichannel sieve electrode for nerve regeneration applications”, PhD dissertation, The University of Michigan, Ann Arbor, October 1994

[25] J. Parramon, Internal CNM-GAB document. “Design of ITUBRv1.0 chip”

[26] N.O. Sokal and A.D. Sokal, "Class E, a New Class of High Efficiency Tuned Single-Ended Switching Power Amplifiers", IEEE Journal of Solid-State Circuits, Vol. 10, pp 168-176, June 1975.

[27] F. H. Raab, "Idealized Operation of the class E tuned power amplifier", IEEE Transactions on Circuits and Systems, vol CAS-24, Nº 12, December 1977.

[28] M.K. Kazimierczuk, K. Puczko, "Exact Analysis of Class E Tuned Power Amplifier at any Q and Switch Duty Cycle", IEEE Transactions on Circuits and Systems, Vol. CAS-34, Nº 2, February 1987

[29] P. Troyk, M. Schwan, “Closed-loop class E transcutaneous power and data link for microimplants”, IEEE Transactions on Biomedical Engineering, vol. 39, nº6, Jun’92